

Glucose Modulation of Glucokinase Activation by Small Molecules[†]

Erik C. Ralph, Jim Thomson, Jonathan Almaden, and Shaoxian Sun*

Biochemical Pharmacology, La Jolla Laboratories, Pfizer Global Research and Development, San Diego, California 92121

Received December 21, 2007; Revised Manuscript Received February 15, 2008

ABSTRACT: Small molecule activators of glucokinase (GK) were used in kinetic and equilibrium binding studies to probe the biochemical basis for their allosteric effects. These small molecules decreased the glucose $K_{0.5}$ (~ 1 mM vs ~ 8 mM) and the glucose cooperativity (Hill coefficient of 1.2 vs 1.7) and lowered the k_{cat} to various degrees (62–95% of the control activity). These activators relieved GK's inhibition from glucokinase regulatory protein (GKRP) in a glucose-dependent manner and activated GK to the same extent as control reactions in the absence of GKRP. In equilibrium binding studies, the intrinsic glucose affinity to the activator-bound enzyme was determined and demonstrated a 700-fold increase relative to the apoenzyme. This is consistent with a reduction in apparent glucose K_D and the steady-state parameter $K_{0.5}$ as a result of enzyme equilibrium shifting to the activator-bound form. The binding of small molecules to GK was dependent on glucose, consistent with the structural evidence for an allosteric binding site which is present in the glucose-induced, active enzyme form of GK and absent in the inactive apoenzyme [Kamata et al. (2004) *Structure* 12, 429–438]. A mechanistic model that brings together the kinetic and structural data is proposed which allows qualitative and quantitative analysis of the glucose-dependent GK regulation by small molecules. The regulation of GK activation by glucose may have an important implication for the discovery and design of GK activators as potential antidiabetic agents.

Glucokinase (GK)¹ is one of four known mammalian hexokinases which converts glucose to glucose 6-phosphate and plays a key role in maintaining glucose homeostasis. Since the first report linking GK to glycemic disease was published in 1992 (1), nearly 200 GK inactivating mutations and 5 activating mutations have been identified in maturity-onset diabetes mellitus and hypoglycemia patients, respectively (2). This strongly underscores the significance of GK activity in the regulation of blood glucose levels. GK exerts glucose control largely through its function, which stimulates glucose-dependent insulin secretion in pancreatic β cells and facilitates glucose uptake for conversion to glycogen in the liver. Also known as hexokinase D or IV, GK differs kinetically from the other hexokinases due to its cooperative glucose dependence (Hill coefficient 1.7), low affinity for glucose ($K_{0.5}$ 7–8 mM), and lack of product inhibition by glucose 6-phosphate (2). These kinetic properties allow GK to respond quickly to changes in glucose concentrations under physiological conditions, making GK well suited for its role as a glucose sensor (3).

GK is a monomeric enzyme with one active site; therefore, its kinetic cooperativity with glucose has to be explained via kinetic models as opposed to interactions between multiple subunits. The “mneumonical” (4, 5) and “slow-transition” (6, 7)

models are most commonly presented and are nicely summarized in reference to GK by Cornish-Bowden and Cárdenas (8). Both models involve two conformations of GK that differ in their relative affinities for glucose. The equilibrium distribution between the two conformations is dependent upon the glucose concentration, and the rate of conformational change is slower than the rate of catalysis under steady-state conditions. The inability of the two conformations to come to equilibrium during steady-state catalysis yields the cooperative kinetics. The two models differ in that the enzyme conformation most prevalent at low glucose concentrations is active in the slow-transition model and inactive in the mneumonical model. In 2004, crystal structures were presented for two substantially different conformations of GK with and without glucose bound (9). The conformation obtained in the absence of glucose was determined to be inactive due to the absence of essential residues for enzymatic catalysis at the active site, thus providing support for the mneumonical model.

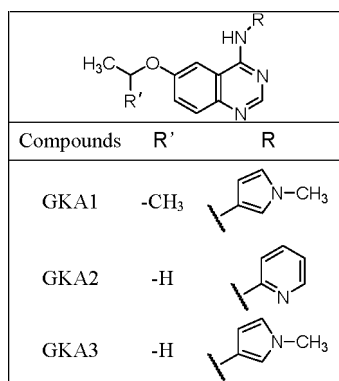
Structural studies have also revealed an allosteric site in glucose-bound GK where small molecules bind (9–12). Importantly, this allosteric site is absent in apo GK (9). These small molecules, referred to as GK activators (GKAs), were reported to increase the enzymatic activity of GK via enhancing the glucose affinity (i.e., lowering $K_{0.5}$) (10, 12–16). In these previous studies, the maximal enzymatic activity (k_{cat}) was either increased or unaffected. A substantial decrease in k_{cat} has not been reported. GKAs are shown to stimulate the insulin secretion in β cells and increase hepatic glucose metabolism *in vitro* (10, 12–14, 16–20). *In vivo*, GKAs lower glucose levels in normal and diabetic animal models. Recently, GKAs were progressed into phase I

[†] This work was supported by the Pfizer Global Research and Development La Jolla Postdoctoral Program.

* To whom correspondence should be addressed. Phone: 858-526-4922. Fax: 858-526-4240. E-mail: shaoxian.sun@pfizer.com.

¹ Abbreviations: GK, glucokinase; GKRP, glucokinase regulatory protein; GKA, glucokinase activator; HEPES, 4-(2-hydroxyethyl)-1-piperazineethanesulfonic acid; DTT, dithiothreitol; TCEP, tris(2-carboxyethyl)phosphine; NADH, reduced nicotinamide adenine dinucleotide; SPA, scintillation proximity assay; ITC, isothermal calorimetry; DMSO, dimethyl sulfoxide; DSC, differential scanning calorimetry.

Scheme 1: Small Molecule Activators of Glucokinase



clinical trials, but the results of GKA efficacy in humans are not yet available. While significant progression has been made with GKAs as a potential therapy for diabetes treatment, the understanding of the fundamental action of GKAs on the enzyme level is still lacking. The goal of the current study is to gain deeper insight into the biochemical mechanism of GK activation by small molecules.

Another important aspect of GKA is the effect on the regulation of GK by GK regulatory protein (GKRP). Hepatic GK activity is inhibited by GKRP via formation of an inactive GK–GKRP complex (21, 22). When the glucose concentration rises, GK dissociates from GKRP. GKAs have been shown to increase hepatic glucose phosphorylation. However, there have been conflicting reports as to whether GKAs disrupt the GK–GKRP complex *in vitro* (13, 16).

In this study, small molecules with different *in vitro* GK activation profiles were examined with regard to their effects on the kinetic parameters of GK and GK–GKRP dissociation. A kinetic model is proposed which provides a qualitative and quantitative analysis of the allosteric effects of activators and their dependence on glucose. In addition, the disruption of the GK–GKRP complex by GKAs in the presence of glucose is confirmed. These observations suggest that glucose is a key modulator for the action of GKAs on GK activity. This study thus provides further understanding of the mechanism of action of GKAs and their potential therapeutic value.

EXPERIMENTAL PROCEDURES

Materials. Glucose, HEPES, pyruvate kinase/lactate dehydrogenase, phosphoenolpyruvate, dithiothreitol (DTT), tris(2-carboxyethyl)phosphine (TCEP), NADH, and ATP were purchased from Sigma (St. Louis, MO). GKA1 is (6-isopropoxyquinazolin-4-yl)(1-methyl-1*H*-pyrazol-3-yl)amine, GKA2 is (6-ethoxyquinazolin-4-yl)pyridin-2-ylamine, and GKA3 is (6-ethoxyquinazolin-4-yl)(1-methyl-1*H*-pyrazol-3-yl)amine. The chemical structures of GKA1–3 are shown in Scheme 1. The YSi copper His-tag beads used in the scintillation proximity assay (SPA) were purchased from Amersham Biosciences, now GE Healthcare (Piscataway, NJ). Data analysis was performed using GraphPad Prism (GraphPad, Inc.) with the exception of the ITC data which used ORIGIN software provided with the instrument.

Protein Expression and Purification. Recombinant human β -cell GK and human GKRP were purified as previously described (23, 24). Briefly, N-terminal His₆-tagged GK and C-terminal FLAG-tagged GKRP were purified from *Escheri-*

chia coli using nickel and FLAG affinity chromatography, respectively, followed by size exclusion chromatography. GK was stored in a buffer containing 25 mM HEPES, 50 mM NaCl, 5 mM DTT, and 5% glycerol, pH 7.5 at –80 °C. GKRP was stored in a buffer containing 25 mM Tris-HCl, 150 mM NaCl, 20% glycerol, and 5 mM DTT, pH 7.4 at –80 °C.

Steady-State Kinetics of GK. GK activity was measured by monitoring the rate of ATP hydrolysis to ADP using the pyruvate kinase/lactate dehydrogenase coupled enzyme system as previously described (23). Assays were run at 25 °C in 50 mM HEPES, 25 mM KCl, 2 mM DTT, 5 mM MgCl₂, 0.7 mM NADH, 4 mM PEP, and 1 unit mL^{–1} PK/LDH, pH 8.0. For experiments where the glucose concentration was varied, the assay buffer contained 2.5 mM ATP. When the ATP concentration was varied, assays contained 50 mM glucose. GKA stock solutions were prepared in DMSO. The final concentration of DMSO in the assays was below 2% (v/v) and had no effect on the GK activity.

Catalytic activity of GK as a function of the glucose concentration exhibited sigmoidal kinetics. The data were fit to the Hill equation (eq 1), where v is the reaction rate normalized to the enzyme concentration, $[Glc]$ is the glucose concentration, $K_{0.5}$ is the glucose concentration at half-maximal activity, and h is the Hill coefficient, which indicates the level of glucose cooperativity. GK displays hyperbolic kinetics with ATP at saturating glucose concentrations, and the data were fit to the Michaelis–Menten equation.

$$v = \frac{K_{cat}[Glc]^h}{K_{0.5}^h + [Glc]^h} \quad (1)$$

GKA potencies for modulation of GK activity, as described by the EC₅₀ values, were determined at various glucose concentrations. The GK activity was plotted as a function of the GKA concentration, and the data were fit to eq 2. Here, v_0 and v_a are the rates obtained in the absence and presence of GKA, respectively, $[A]$ is the GKA concentration, v_m is the rate at saturating GKA concentration, and EC₅₀ is the GKA concentration which yields half the maximal activation or inhibition.

$$v_a = \frac{v_0 + v_m([A]/EC_{50})}{1 + [A]/EC_{50}} \quad (2)$$

The effect of GKAs on the GK–GKRP interaction was also evaluated using the same assay system in the presence of 0.2 μ M GKRP and 5 mM glucose. The GKRP concentration used was sufficient to inhibit approximately 95% of GK's activity in the absence of GKAs. Higher GKRP concentrations were not used, as additional GKRP may have increased GKA EC₅₀ values above the accessible range of concentrations determined by the activators' solubilities. The GKRP was first exchanged from its storage buffer into 25 mM HEPES, 50 mM KCl, 10% glycerol, and 2 mM DTT, pH 8.0, via repeated dilution and reconcentration steps using an Amicon Ultra-15 centrifugal filter. The glycerol was present to help stabilize GKRP; the final concentration of glycerol in the assays was 0.3%. No significant differences in activity were seen between preincubation of GK and GKRP for either 0 or 30 min prior to GKA addition. Control experiments were run under identical condition in the absence

of GKRP. The GK activity was plotted as a function of the GKA concentration, and the data were fit to eq 2.

Activator and Glucose Binding Measured by Calorimetry and SPA. Differential scanning calorimetry (DSC) was used to examine activator binding to GK in the absence and presence of 100 mM glucose. The final concentration of GKA1 and GK was 100 μ M and 0.3 mg mL⁻¹, respectively. The instrument and software details, as well as the experimental setup, were as previously described (23) with two exceptions. Buffer exchange was achieved using a Millipore (Bedford, MA) YM-10 regenerated cellulose column rather than through dialysis, and a simple linear subtraction over the temperature range of 35–40 °C was found to be sufficient for normalizing the observed C_p values. The thermal midpoint of transition (T_m) was defined as the temperature corresponding to the maximum relative C_p value. C_p values were recorded at 0.4 °C intervals.

The apparent binding affinity of GKA1 to GK was determined in the presence of 100 mM glucose by isothermal calorimetry (ITC) at 25 °C. Experiments were run using a MicroCal VP-ITC (Northampton, MA) with a 1.441 mL reaction cell volume. Both GK and GKA1 were prepared in 50 mM Tris, 100 mM KCl, 2 mM TCEP, and 100 mM glucose, pH 8.0. DMSO was added to the GK solution to keep the same DMSO content (1% v/v). The starting concentration of GK (20 μ M) was determined spectrophotometrically using the calculated extinction coefficient of 31150 M⁻¹ cm⁻¹ (23). The GKA1 solution (300 μ M) was injected via the titration syringe in 15 μ L aliquots at approximately 0.8 μ L s⁻¹, with 6 min equilibration time between injections. The data were fit using ORIGIN software provided with the instrument.

Formation of the GK–GKA complex was also monitored at various glucose concentrations using SPA. In this method, His₆-tagged GK was captured on the surface of copper SPA beads that contain scintillant. Binding of ³H-GKA1 to GK brings ³H into close proximity to the beads, resulting in a scintillation signal. Assays were set up in 96-well plates and contained 50 mM HEPES, 25 mM KCl, 5% glycerol, and 14 mM 2-mercaptoethanol, pH 8.0, with 0.1 μ M GK and 0–100 mM glucose. A serial dilution of GKA1 containing 5% or 10% ³H-GKA1 (molar ratio) was added to the wells. Assays contained less than 2% (v/v) DMSO. SPA beads were added last to a final concentration of 1 mg mL⁻¹. The plates were then shaken for 2 min on a plate shaker and incubated for 2 min at 20 °C prior to reading with a TopCount scintillation counter (Packard Biosciences, now PerkinElmer). It was necessary to keep the incubation time short as a time-dependent drift in the scintillation signal and a slight increase in the K_D values were observed under low glucose concentrations (\leq 5 mM). Subsequent analyses of the same samples typically showed reproducibility within 1.5–2-fold over a 10 min time scale. This drift was attributed to instability of GK under these assay conditions.

The nonspecific binding of GKA1 to the SPA beads was measured in the absence of GK and showed a linear relationship to the ³H-GKA1 concentrations, which was subtracted from the enzymatic data. The corrected scintillation signal (CPM) was plotted as a function of the GKA1 concentration and fit to eq 3 to determine the apparent K_D for GKA1. Here, C_{\max} is the maximal CPM, and [E] and [A] are the GK and activator concentrations, respectively.

This equation was chosen over the Langmuir isotherm equation to account for the depletion of free GKA, which occurs when the apparent K_D value is comparable to or smaller than the GK concentration (25).

CPM =

$$C_{\max} \frac{([E] + [A] + K_D) - \sqrt{([E] + [A] + K_D)^2 - 4[E][A]}}{2[E]} \quad (3)$$

The apparent binding affinities for GKA2 and GKA3 were determined by competitive displacement of ³H-GKA1 using SPA. The buffer conditions and enzyme concentrations were as described above. The concentration of GKA1 in the assay was 2 μ M with 10% (molar ratio) ³H-GKA1. The scintillation count (CPM) was plotted versus the nonlabeled GKA concentration and fit to eq 4. Here, [A₁] and K_1 are the concentration and apparent K_D of GKA1, respectively, and [A_n] and K_n are the concentration and apparent K_D value for the nonlabeled GKAs. The K_1 values of 0.21 and 0.14 μ M determined above were used at 5 and 100 mM glucose, respectively.

$$\text{CPM} = C_{\max} \left/ \left(1 + \frac{[A_n]}{K_n(1 + [A_1]/K_1)} \right) \right. \quad (4)$$

Apparent binding affinities for glucose in the presence of GKA were also determined using SPA. Glucose binding to GK increases the apparent binding affinity of ³H-GKA1, leading to an increase in the scintillation signal. Therefore, ³H-GKA1 can serve as a reporter for glucose binding to GK via SPA. A serial dilution of glucose concentrations was added to solutions containing 0.1 μ M GK and 1–20 μ M GKA1 with 10% (molar ratio) ³H-GKA1. The assay conditions and the data analysis were as described above.

GK–GKRP Dissociation Monitored by Size Exclusion Chromatography. The GK–GKRP complex was formed by incubating GK (4 μ M) and GKRP (2 μ M) at room temperature in 25 mM HEPES, pH 7.2, 100 mM KCl, 50 μ M fructose 6-phosphate, and 1 mM DTT for 30 min. The effects of glucose and GKA1 on the GK–GKRP complex were determined by including 50 mM glucose or 10 μ M GKA1 or both in the incubation buffer. A TSK-Gel G3000SW analytical size exclusion column was equilibrated with the same incubation buffer. The protein sample (40 μ L) was then injected onto the column and eluted with the equilibration buffer at a flow rate of 1 mL min⁻¹ for 18 min using a Hitachi D-7000 HPLC. The eluate was monitored by UV absorbance at 280 nm, and peak areas were quantified using the reports manager software provided with the instrument.

RESULTS

Activation of GK Steady-State Kinetics. The small molecule activators were first characterized via the analysis of their effects on various steady-state kinetic parameters of GK. The results are summarized in Table 1. All of the activators tested here decreased the glucose $K_{0.5}$ and Hill coefficient to a similar degree. However, their effects on k_{cat} varied from 62% (GKA2) to 95% (GKA3) of the control in the absence of GKAs. As a result, GKA2 increased GK activity only at glucose concentrations below \sim 7 mM (Figure 1). Incidentally, this is the fasting blood glucose level which defines a diabetic. GKA1 and GKA3 activated GK over a

Table 1: Steady-State Kinetic Parameters of GK with GKAs^a

	k_{cat} (s ⁻¹)	Hill coeff	$K_{0.5,\text{Glc}}$ (mM)	$K_{\text{m,ATP}}$ (mM)	$k_{\text{cat}}/K_{\text{m,ATP}}^b$ (mM ⁻¹ s ⁻¹)
DMSO	55 ± 5	1.7 ± 0.1	7.8 ± 0.5	0.23 ± 0.04	240 ± 30
GKA1	44 ± 2	1.1 ± 0.1	1.3 ± 0.1	0.11 ± 0.01	400 ± 40
GKA2	34 ± 2	1.2 ± 0.1	1.6 ± 0.1	0.10 ± 0.01	330 ± 20
GKA3	52 ± 4	1.3 ± 0.1	1.3 ± 0.1	0.14 ± 0.02	360 ± 30

^a Kinetic assays were run in the absence and presence of 50 μM GKA as described in the Experimental Procedures section. When glucose was varied, the ATP concentration was held at 2.5 mM. The $K_{0.5}$ and Hill values are from fits of the data to eq 1. When ATP was varied, glucose was held at 50 mM. The $K_{\text{m,ATP}}$ and $k_{\text{cat}}/K_{\text{m,ATP}}$ values are from fits of the data to the Michaelis–Menten equation. Values shown are the average of two independent determinations. ^b Values are the average of four independent determinations.

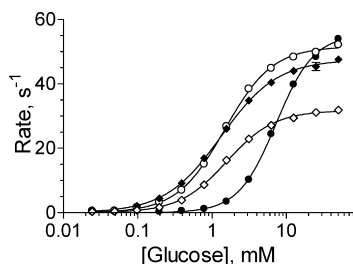


FIGURE 1: Representative data for steady-state kinetic analysis in the absence and presence of 50 μM GKA. The figure is showing the data obtained with the DMSO control (●), GKA1 (◆), GKA2 (◇), and GKA3 (○). Experimental details were as described for Table 1. The assays were done in duplicate. Unless otherwise indicated, the relative error is smaller than the data markers. The data were fit to eq 2.

larger range of glucose, up to approximately 20 mM. The effect of GKAs on the ATP K_{m} was less prominent compared to glucose $K_{0.5}$ with an approximately 2-fold decrease. The pseudo-first-order rate constant $k_{\text{cat}}/K_{\text{ATP}}$ was slightly increased from 240 mM⁻¹ s⁻¹ to 330–400 mM⁻¹ s⁻¹.

The GKA effects on the apparent glucose binding affinities, as described by the $K_{\text{D,Glc}}$ values, were determined in the absence of ATP using SPA. This method is preferred over the protein tryptophan fluorescence method for glucose binding (23) as it requires significantly less enzyme (0.1 vs 10 μM) and thereby allows for the apparent $K_{\text{D,Glc}}$ determinations at low micromolar GKA concentrations. Values determined at 20 μM GKA1 were in reasonable agreement between the two methods (57 ± 14 μM by SPA vs 78 ± 17 μM by fluorescence). Compared to glucose $K_{0.5}$, apparent glucose $K_{\text{D,Glc}}$ was more sensitive to the activator concentrations with nearly 100-fold change over 0–20 μM GKA1 (Figure 2).

Glucose Dependence of GKA Binding to GK. The binding of GKA1 to GK in the absence and presence of glucose was first monitored by DSC. In DSC, specific binding of a ligand to protein is predicted to increase the observed transition temperature of protein unfolding (T_{m}) (26). Representative DSC curves are shown in Supporting Information (SI) Figure 1. Addition of glucose to apo GK increased the observed T_{m} from 47.9 ± 0.4 to 50.5 ± 0.1 °C. These T_{m} values are in excellent agreement with previous determinations (23). Addition of GKA1 to the apoenzyme did not significantly shift the T_{m} value (48.2 ± 0.2 °C). In contrast, addition of GKA1 in the presence of saturating glucose

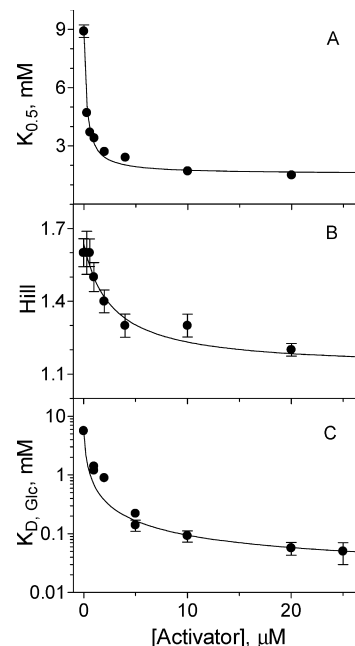


FIGURE 2: Glucose $K_{0.5}$, Hill coefficient, and $K_{\text{D,Glc}}$ values as a function of GKA1 concentration. All assays were done in duplicate. Unless otherwise indicated, the relative error is smaller than the data markers. The glucose $K_{0.5}$ (A) and Hill coefficient (B) were determined by the steady-state kinetics of GK. (A, B) Trend lines were drawn for visual purposes only. (C) Apparent glucose $K_{\text{D,Glc}}$ values were determined in the absence of ATP by SPA as described in the Experimental Procedures section. The zero activator value is from ref 23. The line shows the fit of the $K_{\text{D,Glc}}$ data to eq 5 using 5 mM for the $K_{\text{D,Glc}}$ in the absence of GKA and 0.14 μM for the term $K_2K_5 + K_5$.

concentration increased the T_{m} to 55.7 ± 0.1 °C. These results suggest that glucose is required for GKA binding to GK.

The apparent $K_{\text{D,GKA}}$ in the presence of glucose was determined by ITC and SPA. In the ITC study, the $K_{\text{D,GKA1}}$ value was determined as 0.09 μM at 100 mM glucose, with a GKA/GK molar ratio of 0.8 (SI Figure 2). This is consistent with the $K_{\text{D,GKA1}}$ value of 0.14 μM obtained by direct titration of GKA1 using SPA. Since it requires significantly less protein and has higher throughput than ITC, the SPA method was utilized to determine the GKA binding affinity at various glucose concentrations.

In the absence of glucose, no binding of GKA1 was observed using the SPA method, consistent with the DSC results (SI Figure 3). Both $K_{\text{D,GKA1}}$ and EC_{50} for GKA1 decreased with glucose concentrations and reached a plateau (Figure 3). The apparent $K_{\text{D,GKA}}$ and EC_{50} values obtained at 5 and 100 mM glucose are summarized in Table 2 for all three GKAs. The K_{D} values determined for GKA1 through the competition method are in good agreement with the values determined through direct titration (Table 2). Increasing the glucose concentration from 5 to 100 mM has little effect on the $K_{\text{D,GKA}}$. In contrast, the EC_{50} values decreased approximately an order of magnitude over the same range of glucose concentrations.

Determination of Intrinsic Binding Affinities for Glucose and Activators. Scheme 2 shows the binding equilibrium between glucose, activator, and GK. Here, A and Glc represent the activator and glucose, respectively, and E*, E, and E_A represent the inactive, active, and activator-bound

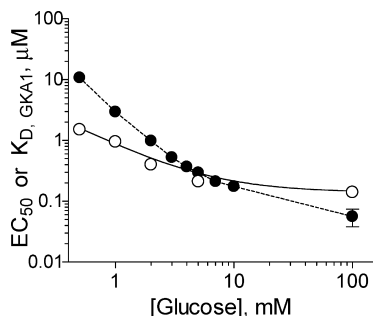


FIGURE 3: Glucose dependence of GKA1 EC_{50} (●) and apparent $K_{D,GKA1}$ values (○). Unless otherwise noted, the relative error is smaller than the data markers. The EC_{50} values were determined by steady-state kinetics of GK. The dashed line connecting the data points was drawn for visual purposes only. The $K_{D,GKA}$ values were determined by SPA. The solid line represents the predicted $K_{D,GKA1}$ values based on eq 6 as described in the Results section.

forms of GK, respectively. On the basis of the structural evidence that the allosteric site is absent in the inactive E^* form (9), GKAs only bind to the active E or $E \cdot \text{Glc}$ enzyme forms. These are the minimal GK forms present in the equilibrium predicted by the mneumonical mechanism (4, 5). K_1 – K_7 refer to the various equilibrium constants. K_1 , K_4 , and K_7 are the dissociation constants for glucose from the $E^* \cdot \text{Glc}$, $E \cdot \text{Glc}$, and $E_A \cdot \text{Glc}$ forms of GK, respectively. K_5 and K_6 are the dissociation constants for GKA from the $E_A \cdot \text{Glc}$ and E_A forms, and K_2 and K_3 are the equilibrium constants for the enzyme isomerization from $E \cdot \text{Glc}$ to $E^* \cdot \text{Glc}$ and E to E^* , respectively.

According to Scheme 2, the apparent $K_{D,Glc}$ can be expressed as a function of the GKA concentration ($[A]$), as shown in eq 5. Similarly, the apparent $K_{D,GKA}$ can be defined as a function of the glucose concentration ($[\text{Glc}]$) as shown in eq 6. Using these two equations, the equilibrium constants were determined as follows for GKA1. Values for K_1 and K_2 (14 ± 2 mM and 0.62 ± 0.05 , respectively) were previously obtained by transient kinetic studies of glucose binding with the assumption that the thermodynamically favored E^* is the predominant enzyme form in the absence of glucose ($K_3 \gg 1$) (23). On the basis of eq 6, the term $K_2K_5 + K_5$ defines the apparent $K_{D,GKA1}$ value at saturating glucose concentrations determined above (0.14 ± 0.01 μM at 100 mM glucose). This allowed for the calculation of 0.09 ± 0.01 μM for K_5 . A fit of the apparent $K_{D,Glc}$ data to eq 5 using 5 mM for the $K_{D,Glc}$ value in the absence of GKA (23) and 0.14 μM for $K_2K_5 + K_5$ yielded the K_7 value of 21 μM with a fitting error of 11 μM . This K_7 value is close to the $K_{D,Glc}$ value of 17 ± 2 μM measured at 100 μM GKA1 using the fluorescence method previously described (23), as expected from eq 5. Similar values of 12 ± 5 and 27 ± 18 were seen with GKA2 and GKA3, respectively, using the same fluorescence method. The values are the average of two independent determinations.

$$\text{apparent } K_{D,Glc} = \frac{\frac{K_1K_2 + K_4}{1 + K_2} + K_7 \left(\frac{[A]}{K_2K_5 + K_5} \right)}{1 + \frac{[A]}{K_2K_5 + K_5}} \quad (5)$$

$$\text{apparent } K_{D,GKA} = \frac{(K_3K_6 + K_6) + (K_2K_5 + K_5) \frac{[\text{Glc}]}{K_7}}{1 + \frac{[\text{Glc}]}{K_7}} \quad (6)$$

No GKA binding was observed in the absence of glucose using both SPA and DSC methods, consistent with a relatively large value (>30 μM) for the term $K_3K_6 + K_6$ in eq 6. Under the assumption of $K_3 \gg 1$, the term $K_3K_6 + K_6$ can be approximated by K_3K_6 . The value of K_3K_6 is calculated as 40 ± 20 μM from K_1 , K_2 , K_5 , and K_7 based on the thermodynamic correlation $K_1K_2K_5 = K_3K_6K_7$. The apparent $K_{D,GKA}$ values predicted by eq 6 using the equilibrium constants determined above agree well with the experimental data (solid line in Figure 3), lending strong support to the mechanism shown in Scheme 2.

Disruption of the GK–GKRP Complex. The ability of GKAs to disrupt the GK–GKRP complex was probed via size exclusion chromatography. The protein elution profile is shown in Figure 4. The GK–GKRP complex (MW 123 kDa) eluted at 8.5 min, while free GK and GKRP (MW 55 and 68 kDa, respectively) coeluted later at 9.8 min. The separation of the two elution peaks was sufficient to allow for a quantitative fitting of peak areas. An increase in the ratio of monomer/dimer peak area is indicative of the disruption of the GK–GKRP complex. Inclusion of GKA1 alone had no significant effect on the monomer/dimer ratio [(1.1 ± 0.1) -fold], while inclusion of glucose in the absence of GKA1 increased the monomer/dimer peak ratio slightly [(1.3 ± 0.1) -fold]. When both glucose and GKA1 were added, there was a large shift in the monomer/dimer distribution of (3.7 ± 0.3) -fold. This suggests that glucose is required for the dissociation of GK–GKRP by GKA. A similar observation was recently reported with an immunoprecipitation assay (16).

The effect of GKAs on the GK–GKRP interaction (18) was also addressed through steady-state kinetic studies. GKA1 not only completely relieved GK inhibition from GKRP but further increases the rate of turnover to achieve an identical maximal rate as in the absence of GKRP (Figure 5). Similar results were seen with other GKAs. The GKA EC_{50} values increase approximately an order of magnitude in the presence of GKRP for GKA1–3 (SI Table 1). Similarly, the GKRP inhibition potency decreases in the presence of GKA (data not shown).

DISCUSSION

Glucose homeostasis is tightly controlled in the body via multiple mechanisms in tissues that sense and respond to the changes in glucose levels between fasting and fed stages. Hyperglycemia in type 2 diabetes is characterized by insufficient insulin secretion to overcome the insulin resistance in the body and increased hepatic glucose production. GK is expressed in pancreatic β cells, liver, gut, and brain and plays a critical role in insulin secretion from β cells, hepatic glucose metabolism, and endocrine glucose sensing. The recent discovery of small molecule activators for GK represents a promising and novel therapy for the treatment of type 2 diabetes since it targets both important tissues of β cells and liver in glucose control. To date, all reported small molecule GK activators decrease the glucose $K_{0.5}$, and

Table 2: GKA EC₅₀ and K_D Values at 5 and 100 mM Glucose^a

	5 mM glucose		100 mM glucose	
	K _{D,GKA} (μM)	EC ₅₀ (μM)	K _{D,GKA} (μM)	EC ₅₀ (μM)
GKA1	0.21 ± 0.04 (2) 0.21 ± 0.06 (3) ^b	0.47 ± 0.13 (4)	0.20 ± 0.03 (3) 0.14 ± 0.01 (2) ^b	0.056 ± 0.018 (3)
GKA2	0.38 ± 0.06 (4)	1.6 ± 0.4 (4)	0.27 ± 0.05 (4)	0.25 ± 0.06 (3)
GKA3	0.9 ± 0.2 (4)	1.4 ± 0.4 (4)	0.59 ± 0.03 (3)	ND ^c

^a EC₅₀ values were determined by measuring the rate of steady-state turnover. Unless indicated, K_{D,GKA} values were determined using competitive ligand displacement SPA with ³H-GKA1. The table shows averaged values followed by the standard deviation and the number of independent determinations. ^b These K_{D,GKA} values were determined by direct titration of GKA1 at 5 and 100 mM glucose, respectively, and subsequently used in the calculation of K_{D,GKA} values for GKA1–3 according to eq 4. ^c This EC₅₀ value was not well determined due to the minimal effect of GKA3 on GK activity at 100 mM glucose.

Scheme 2: Equilibrium Binding of Glucose (Glc) and Activators (A) to GK



some of them increase the *k*_{cat} while others have no effect on *k*_{cat}. This present study introduces a novel activation profile with a decreased *k*_{cat} as exemplified by GKA2. Since GKAs have similar effects on the glucose K_{0.5} value, their differential effects on *k*_{cat} define the glucose concentration at which GKAs no longer activate but instead inhibit enzyme activity. The biochemical basis for the different activation profiles and their pharmacological implications is intriguing and may provide valuable information for the design and development of GK modulators as an antidiabetic therapy.

The ability to lower the kinetically determined glucose K_{0.5} value is a defining characteristic of all GKAs. We

therefore determined the effect of GKAs on the glucose binding affinity under equilibrium conditions in the absence of ATP. By selectively binding the active enzyme conformations, activators shift the enzyme equilibrium away from the E* form to the E_A form (Scheme 2). The E_A form has a 700-fold increase in glucose affinity (K₇ = 21 μM) relative to the E* form (K₁ = 14000 μM) (23), leading to an increase in the overall glucose binding as predicted by eq 5. Although the current data do not allow for a quantitative comparison of glucose affinities for the E and E_A forms of GK (K₄ vs K₇), some further observations are noted in this study. The K_{D, Glc} values determined at 100 μM GKA concentrations are similar for all three GKAs, independent of the GKA structure. This may suggest that the glucose affinity for the E_A form of the enzyme is similar to the glucose affinity for the E form. This possibility is supported by the observation that crystal structures for the E_A·Glc and E·Glc forms of GK are nearly identical (11). Assuming the same glucose affinities for the E and E_A forms (K₄ = K₇) allows for the calculation of a value of 440 for K₃ from the thermodynamic relationship K₁K₂ = K₃K₄. This large value of K₃ is consistent with the results presented in this study, implying a strong thermodynamic preference for the inactive E* form of GK in the absence of glucose.

A preexisting equilibrium between the inactive and active GK in the absence of glucose was reported for the liver GK isoform, which suggested a small but significant fraction of active apoenzyme (27). We were not able to detect an active enzyme E form in the absence of glucose with the β-cell GK isoform. We observed a protein fluorescence change upon addition of ATP in the absence of glucose (28) similar to the report with liver GK in their characterization of ATP analogue binding to the active and inactive enzyme forms. However, this is likely due to a quenching effect by ATP, since no specific binding of ATP was observed by calorimetry in the absence of glucose (23). The transient kinetic studies of glucose binding with β-cell GK showed biphasic kinetics when data were collected on a log scale to capture the rapid first phase, in contrast to the monophasic kinetics reported for liver GK. These differences in experimental techniques and subsequent data analysis likely contribute to the different conclusions. However, although the GK isoforms have been shown to have similar steady-state kinetics and interactions with GKR (29, 30), the possibility of small differences in the apoenzyme equilibrium between E and E* cannot be ruled out.

The kinetic model for glucose and activator binding in Scheme 2 can now be further extended to include the ATP binding and subsequent enzyme catalysis to describe the

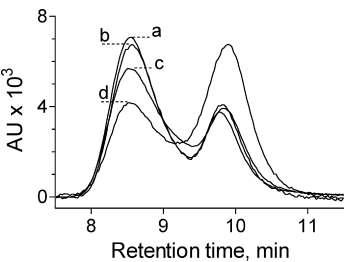


FIGURE 4: Elution profiles of GK, GKR, and the GK-GKR complex from size exclusion HPLC. Profiles were obtained in the absence of glucose and GKA1 (a) or the presence of 10 μM GKA1 (b), 50 mM glucose (c), or both (d). The eluate was monitored by UV absorbance at 280 nm. The earlier peak is attributed to the GK-GKR complex, while the latter peak represents both free monomers of GK and GKR.

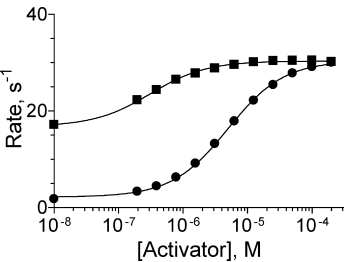


FIGURE 5: GK activation by GKA1 in the absence (■) or presence (●) of 0.2 μM GKR. Assay conditions were as described in the Experimental Procedures section. Concentrations of GKA1 in the assay were varied from 0.2 to 200 μM, and the DMSO control was shown here as 10⁻⁸ M. Assays were done in duplicate. The error bar is smaller than the data markers. The lines are the fit of the data to eq 2.

to physiologically relevant glucose levels is sufficient to reduce the hypoglycemia risk.

The *in vitro* activation profile of GKAs describes the modulation of GK activity at various concentrations of glucose. Compounds that increase activity at all glucose concentrations (higher k_{cat}) are expected to stimulate insulin secretion in the β cells and increase glucose uptake in the liver. In contrast, compounds such as GKA2 which decrease the k_{cat} may lead to a less profound effect on insulin stimulation in β cells. However, these molecules are still able to dissociate GGRP from GK and thereby provide benefit by increasing the level of active GK in the liver. Together, the overall moderate level of activation might be beneficial in reducing the risk of hypoglycemia. Further study is necessary to define an activation profile that minimizes the hypoglycemia risk while retaining efficacy.

In summary, small molecule activators bind to an allosteric site in the active form of GK and shift the enzyme equilibrium from an inactive enzyme form with low glucose affinity to an active form with high glucose affinity. As a result, the overall glucose binding is increased. The binding of activator is dependent on glucose which induces a large conformational change to form the allosteric site in GK. The interdependence of glucose and activators represents an important aspect of the allosteric regulation of GK, which may have a significant implication in the development of small molecule activators as potential antidiabetic agents.

ACKNOWLEDGMENT

We thank Erin Garcia for assistance in the purification of GGRP and Ted Johnson, Wei-Guo Sun, and Chengyu Liu for the chemistry support. We also thank Tom Carlson for expert help in SPA assays, Wei Han Wang for contributions toward this project, Steve Grant for critical reading of the manuscript and insightful discussion, and Peter Oates and Shenping Liu for valuable input.

SUPPORTING INFORMATION AVAILABLE

Figures showing the representative traces for the DSC experiments, data for $K_{\text{D,GKA}}$ determinations by ITC and SPA, a table of kinetic parameters regarding GGRP inhibition, representative structures of previously published GKAs, appendices showing derivations of eqs 5 and 6, and details regarding the kinetic simulation. This material is available free of charge via the Internet at <http://pubs.acs.org>.

REFERENCES

1. Froguel, P. H., Vaxillaire, M., Sun, F., Velho, G., Zouali, H., Butel, M. O., Lesage, S., Vionnet, N., Clement, K., Fougerousse, F., Tanizawa, Y., Weissenbach, J., Beckmann, J. S., Lathrop, G. M., Passa, P. H., Permutt, M. A., and Cohen, D. (1992) Close linkage of glucokinase locus on chromosome 7p to early-onset non-insulin-dependent diabetes mellitus. *Nature* 356, 162–164.
2. Magnuson, M. A., and Matschinsky, F. M. (2004) Glucokinase as a glucose sensor: Past, present, and future, in *Glucokinase and Glycemic Disease: From Basics to Novel Therapeutics* (Matschinsky, F. M., and Magnuson, M. A., Eds.) pp 1–17, Karger, Basel.
3. Matschinsky, F. M., and Davis, E. A. (1998) The distinction between “glucose setpoint”, “glucose threshold” and “glucose sensor” is critical for understanding the role of the pancreatic β -cell in glucose homeostasis, in *Molecular and Cell Biology of Type 2 Diabetes and Its Complications* (Belfiore, F., Lorenzi, M., Molinatti, G. M., and Porta, M., Eds.) pp 14–29, Karger, Basel.
4. Ricard, J., Meunier, J. C., and Buc, J. (1974) Regulatory behavior of monomeric enzymes. 1. The mnemonical enzyme concept. *Eur. J. Biochem.* 49, 195–208.
5. Meunier, J. C., Buc, J., Navarro, A., and Ricard, J. (1974) Regulatory behavior of monomeric enzymes. 2. A wheat-germ hexokinase as a mnemonical enzyme. *Eur. J. Biochem.* 49, 209–223.
6. Neet, K. E., and Ainslie, G. R., Jr. (1980) Hysteretic enzymes. *Methods Enzymol.* 64, 192–226.
7. Ainslie, G. R., Jr., Shill, J. P., and Neet, K. E. (1972) Transients and cooperativity. A slow transition model for relating transients and cooperative kinetics of enzymes. *J. Biol. Chem.* 247, 7088–7096.
8. Cornish-Bowden, A., and Cardenas, M. L. (2004) Glucokinase: A monomeric enzyme with positive cooperativity, in *Glucokinase and Glycemic Disease: From Basics to Novel Therapeutics* (Matschinsky, F. M., and Magnuson, M. A., Eds.) pp 125–134, Karger, Basel.
9. Kamata, K., Mitsuya, M., Nishimura, T., Eiki, J., and Nagata, Y. (2004) Structural basis for allosteric regulation of the monomeric allosteric enzyme human glucokinase. *Structure* 12, 429–438.
10. Grimsby, J., Sarabu, R., Corbett, W. L., Haynes, N. E., Bizzarro, F. T., Coffey, J. W., Guertin, K. R., Hilliard, D. W., Kester, R. F., Mahaney, P. E., Marcus, L., Qi, L., Spence, C. L., Teng, J., Magnuson, M. A., Chu, C. A., Dvorozniak, M. T., Matschinsky, F. M., and Grippo, J. F. (2003) Allosteric activators of glucokinase: potential role in diabetes therapy. *Science* 301, 370–373.
11. Dunten, P., Swain, A., Kammlott, U., Crowther, R., Lukacs, C. M., Levin, W., Reik, L., Grimsby, J., Corbett, W. L., Magnuson, M. A., Matschinsky, F. M., and Grippo, J. F. (2004) Crystal structure of human liver glucokinase bound to a small molecule activator, in *Glucokinase and Glycemic Disease: From Basics to Novel Therapeutics* (Matschinsky, F. M., and Magnuson, M. A., Eds.) pp 145–154, Karger, Basel.
12. Efanov, A. M., Barrett, D. G., Brenner, M. B., Briggs, S. L., Delaunoy, A., Durbin, J. D., Giese, U., Guo, H., Radloff, M., Gil, G. S., Sewing, S., Wang, Y., Weichert, A., Zaliani, A., and Gromada, J. (2005) A novel glucokinase activator modulates pancreatic islet and hepatocyte function. *Endocrinology* 146, 3696–3701.
13. Brocklehurst, K. J., Payne, V. A., Davies, R. A., Carroll, D., Vertigan, H. L., Wightman, H. J., Aiston, S., Waddell, I. D., Leighton, B., Coghlan, M. P., and Agius, L. (2004) Stimulation of hepatocyte glucose metabolism by novel small molecule glucokinase activators. *Diabetes* 53, 535–541.
14. Castelano, A. L., Dong, H., Fyfe, M. C., Gardner, L. S., Kamikozawa, Y., Kurabayashi, S., Nawano, M., Ohashi, R., Procter, M. J., Qiu, L., Rasamison, C. M., Schofield, K. L., Shah, V. K., Ueta, K., Williams, G. M., Witter, D., and Yasuda, K. (2005) Glucokinase-activating ureas. *Bioorg. Med. Chem. Lett.* 15, 1501–1504.
15. Sagen, J. V., Odili, S., Bjorkhaug, L., Zelent, D., Buettger, C., Kwagh, J., Stanley, C., Dahl-Jorgensen, K., de Beaufort, C., Bell, G. I., Han, Y., Grimsby, J., Taub, R., Molven, A., Sovik, O., Njolstad, P. R., and Matschinsky, F. M. (2006) From clinicogenetic studies of maturity-onset diabetes of the young to unraveling complex mechanisms of glucokinase regulation. *Diabetes* 55, 1713–1722.
16. Futamura, M., Hosaka, H., Kadotani, A., Shimazaki, H., Sasaki, K., Ohya, S., Nishimura, T., Eiki, J., and Nagata, Y. (2006) An allosteric activator of glucokinase impairs the interaction of glucokinase and glucokinase regulatory protein and regulates glucose metabolism. *J. Biol. Chem.* 281, 37668–37674.
17. Johnson, D., Shepherd, R. M., Gill, D., Gorman, T., Smith, D. M., and Dunne, M. J. (2007) Glucose-dependent modulation of insulin secretion and intracellular calcium ions by GKA50, a glucokinase activator. *Diabetes* 56, 1694–1702.
18. Fyfe, M. C., White, J. R., Taylor, A., Chatfield, R., Wargent, E., Printz, R. L., Sulpice, T., McCormack, J. G., Procter, M. J., Reynet, C., Widdowson, P. S., and Wong-Kai-In, P. (2007) Glucokinase activator PSN-GK1 displays enhanced antihyperglycaemic and insulinotropic actions. *Diabetologia* 50, 1277–1287.
19. McKerrecher, D., Allen, J. V., Caulkett, P. W., Donald, C. S., Fenwick, M. L., Grange, E., Johnson, K. M., Johnstone, C., Jones, C. D., Pike, K. G., Rayner, J. W., and Walker, R. P. (2006) Design of a potent, soluble glucokinase activator with excellent in vivo efficacy. *Bioorg. Med. Chem. Lett.* 16, 2705–2709.
20. Coope, G. J., Atkinson, A. M., Allott, C., McKerrecher, D., Johnstone, C., Pike, K. G., Holme, P. C., Vertigan, H., Gill, D., Coghlan, M. P., and Leighton, B. (2006) Predictive blood glucose lowering efficacy by glucokinase activators in high fat fed female Zucker rats. *Br. J. Pharmacol.* 149, 328–335.

21. van Schaftingen, E., and Veiga da Cunha, M. (2004) Discovery and role of glucokinase regulatory protein, in *Glucokinase and Glycemic Disease: From Basics to Novel Therapeutics* (Matschinsky, F. M., and Magnuson, M. A., Eds.) pp 193–207, Karger, Basel.
22. Baltrusch, S., and Tiedge, M. (2006) Glucokinase regulatory network in pancreatic B-cells and liver. *Diabetes* 55, S55–S64.
23. Heredia, V. V., Thomson, J., Nettleton, D., and Sun, S. (2006) Glucose-induced conformational changes in glucokinase mediate allosteric regulation: transient kinetic analysis. *Biochemistry* 45, 7553–7562.
24. Heredia, V. V., Carlson, T. J., Garcia, E., and Sun, S. (2006) Biochemical basis of glucokinase activation and the regulation by glucokinase regulatory protein in naturally occurring mutations. *J. Biol. Chem.* 281, 40201–40207.
25. Copeland, R. A. (2000) Protein-ligand binding equilibria, in *Enzymes: A Practical Introduction to Structure, Mechanism, and Data Analysis*, 2nd ed., pp 76–108, Wiley-VCH, New York.
26. Sturtevant, J. M. (1987) Biochemical applications of differential scanning calorimetry. *Annu. Rev. Phys. Chem.* 38, 463–488.
27. Kim, Y. B., Kalinowski, S. S., and Marcinkeviciene, J. (2007) A pre-steady state analysis of ligand binding to human glucokinase: evidence for a preexisting equilibrium. *Biochemistry* 46, 1423–1431.
28. Heredia, V. V., and Sun, S., unpublished results.
29. Veiga-da-Cunha, M., Xu, L. Z., Lee, Y. H., Marotta, D., Pilkis, S. J., and Van Schaftingen, E. (1996) Effect of mutations on the sensitivity of human beta-cell glucokinase to liver regulatory protein. *Diabetologia* 39, 1173–1179.
30. Tiedge, M., Krug, U., and Lenzen, S. (1997) Modulation of human glucokinase intrinsic activity by SH reagents mirrors post-translational regulation of enzyme activity. *Biochim. Biophys. Acta* 1337, 175–190.
31. Storer, A. C., and Cornish-Bowden, A. (1977) Kinetic evidence for a “mnemonic” mechanism for rat liver glucokinase. *Biochem. J.* 165, 61–69.
32. Monasterio, O., and Cardenas, M. L. (2003) Kinetic studies of rat liver hexokinase D (“glucokinase”) in non-co-operative conditions show an ordered mechanism with MgADP as the last product to be released. *Biochem. J.* 371, 29–38.

BI702516Y